BJ www.biochemj.org

BJ Structure

Biochem. J. (2010) **426**, 197–203 (Printed in Great Britain) doi:10.1042/BJ20091612

online commentary

Iron-binding activity in yeast frataxin entails a trade off with stability in the $\alpha 1/\beta 1$ acidic ridge region

Ana R. CORREIA*, Tao WANG†[1], Elizabeth A. CRAIG† and Cláudio M. GOMES*[2]

*Instituto Tecnologia Química e Biológica, Universidade Nova de Lisboa, Av. República 127, 2780-756 Oeiras, Portugal, and †Department of Biochemistry, University of Wisconsin, Madison, WI 53706, U.S.A.

Frataxin is a highly conserved mitochondrial protein whose deficiency in humans results in Friedreich's ataxia (FRDA), an autosomal recessive disorder characterized by progressive ataxia and cardiomyopathy. Although its cellular function is still not fully clear, the fact that frataxin plays a crucial role in Fe–S assembly on the scaffold protein Isu is well accepted. In the present paper, we report the characterization of eight frataxin variants having alterations on two putative functional regions: the $\alpha 1/\beta 1$ acidic ridge and the conserved β-sheet surface. We report that frataxin iron-binding capacity is quite robust: even when five of the most conserved residues from the putative iron-binding region are altered, at least two iron atoms per monomer can be bound, although with decreased affinity. Furthermore, we conclude that the acidic ridge is designed to favour function over stability. The negative charges have a functional role, but at the same time significantly impair frataxin's stability. Removing five of those charges results in a thermal stabilization of $\sim 24\,^{\circ}C$ and reduces the inherent conformational plasticity. Alterations on the conserved β-sheet residues have only a modest impact on the protein stability, highlighting the functional importance of residues 122–124.

Key words: frataxin, iron–sulfur cluster, Isu, metallochaperone, protein folding, Yfh1.

INTRODUCTION

Reduced expression of frataxin, or in some cases, expression of frataxin variants, leads to the development of Friedreich's ataxia (FRDA), an autosomal recessive neurodegenerative and cardiodegenerative disease characterized by progressive ataxia and cardiomyopathy [1–3]. In spite of the availability of multicellular models for the disease [4,5], insights into possible therapeutic strategies [6,7] and broader systematic clinical studies [8], the pathogenesis of FRDA and its relationship with frataxin remains to be fully understood. Frataxin is a highly conserved protein localized in the mitochondria whose function is associated with iron homoeostasis. Frataxin deficiency, as shown recently using conditional knockout mice, down-regulates molecules involved in mitochondrial iron-utilization pathways (Fe–S cluster and haem biosynthesis, and iron storage), while cellular iron uptake and its availability for mitochondrial uptake are increased [5]. This illustrates the complex interplay between frataxin deficiency and iron homoeostasis in the context of FRDA [5].

The human and yeast frataxin (Yfh1) orthologues have a high degree of amino acid (65 %) and structural identity. The phenotype observed as a consequence of frataxin's deficiency is very similar in human and yeast cells [9,10]. Hence, the yeast model system has been used frequently to study frataxin's function, as well as the pathological events associated with FRDA. Although a detailed understanding of frataxin function is still lacking, data suggest a role as an iron metallochaperone [11–14], delivering iron to its binding partners, promoting haem and Fe–S clusters biosynthesis, as well as Fe–S cluster repair [15–17]. Although, initially, oligomerization was believed to be dispensable *in vivo*, it has been shown subsequently that oligomerization impairment is harmful under oxidative stress conditions and it leads to a decrease in yeast chronological lifespan [11,18,19]. Yfh1 is not essential, but its absence causes severe growth defects and a reduction in the activity of Fe–S-cluster-containing enzymes, such as aconitase [9,10,19,20]. Iron binding by frataxins, a requirement for a role as a metallochaperone, has been well documented by several laboratories [16,21,22]. Frataxins bind iron with micromolar binding affinities, but different stoichiometries: while monomeric human frataxin binds six or seven iron ions ($K_d \sim 12$–$55\ \mu M$ [16]), monomeric frataxin from *Drosphila* binds one ferrous iron ($K_d \sim 6\ \mu M$ [22]) and yeast frataxin binds two ferrous irons ($K_d \sim 2.5\ \mu M$ [21]). This variability suggests a certain plasticity of the frataxin fold in respect to binding iron. In fact, an NMR-based investigation of the iron binding to Yfh1 at low stoichiometry (up to 2:1 Fe/Yfh1) denoted changes in ten distinct residues [23], which could indicate long-range effects upon iron binding, or lower-affinity sites. More complex effects arise at higher Fe/Yfh1 stoichiometries. Like human frataxin, Yfh1 undergoes iron-dependent oligomerization, above a threshold of two irons per monomer, according to the progression $\alpha \rightarrow \alpha_3 \rightarrow \alpha_6 \rightarrow \alpha_{12} \rightarrow \alpha_{24} \rightarrow \alpha_{48}$ [11,18]. This property has been established as important for iron-induced oxidative stress protection, but not for Fe–S cluster biogenesis [19,24].

The conserved frataxin fold consists of an α/β sandwich motif, with two α-helices (N- and C-terminal) that construct the helical plane and five antiparallel β-strands that form the β-sheet plane. A sixth (seventh in the human protein) β-strand intersects the helical and β-sheet planes [23,25–28]. The first helix ($\alpha 1$) and the edge of the first β-strand ($\beta 1$) form a semi-conserved acidic ridge that constitutes the putative iron-binding region of the protein [21,23,28]. A set of conserved residues in the β-sheet surface constitutes the other putative functional region of the protein, believed to be involved in the binding of frataxin to its protein partners [23,29]. Recently, we have shown that

Abbreviations used: FRDA, Friedreich's ataxia; IPTG, isopropyl β-D-thiogalactoside; −ura DO, uracil drop-out.

[1] Present address: Hillman Cancer Institute, University of Pittsburgh, Pittsburgh, PA 15213, U.S.A.

[2] To whom correspondence should be addressed (email gomes@itqb.unl.pt).

mutations at the conserved β-sheet residues 122–124 affect neither iron-binding capacity nor the oligomerization properties of frataxin, although these mutations do compromise the interaction with Isu [30].

To complement previous functional characterization of *YFH1* mutants, in the present study we address the structural and conformational effects of eight functional mutants in yeast frataxin that alter either the acid ridge or conserved residues on the β-sheet surface. We found that the negatively charged residues in the acid ridge that are important for iron binding reduce Yfh1's stability, indicating a trade off between functionality and stability. In addition, alterations in the conserved residues of the portion of the acid ridge found in the β-sheet affected interaction with the scaffold protein Isu, but did not compromise overall protein stability.

EXPERIMENTAL

Yeast strains, plasmids and media

Saccharomyces cerevisiae strains carrying *YFH1* mutant or wild-type genes on plasmids were created by sporulation and dissection of *YFH1*/*yfh1*Δ (W303 background) transformed with the plasmids. *YFH1* mutants were generated by site-directed mutagenesis using pCM189-YFH1 as a template, having *YFH1* under the control of the *tetO* promoter [31]. Constructs containing the following mutations were prepared: yfh1-D86A/E90A/E93A, yfh1-D101A/E103A, yfh1-D86A/E90A/E93A/D101A/E103A, yfh1-N122A, yfh1-N122K (corresponding to the human clinical mutation N146K), yfh1-K123T, yfh1-Q124A and yfh1-N122A/K123T/Q124A. Doxycycline was used at 1 μg/ml to reduce expression. Cells were grown in minimal synthetic medium with −ura DO (uracil drop-out) at 30 °C for 2 days.

Aconitase activity in isolated mitochondria

Mitochondria were isolated, according to the method described in [32], from cells grown in synthetic minimal medium (−ura DO), in the absence of doxycycline. Aconitase activity was measured in isolated mitochondria by monitoring the decrease in the absorbance of the substrate isocitrate at 240 nm as described in [33].

Gene expression and protein purification

The mature form of Yfh1 (amino acids 52–174) with an N-terminal His_6 tag and a thrombin cleavage site in between was cloned into pET-3a vector (Novagen) [19]. Protein expression was induced over 3 h at 37 °C in BL21(DE3) *Escherichia coli* cells by adding IPTG (isopropyl β-D-thiogalactoside) at a final concentration of 0.5 mM. With the exception of Yfh1-K123T, which was expressed at much lower levels (approx. 30 %), all other mutant variants had expression levels identical with those of the wild-type Yfh1. The reduced expression levels of Yfh1-K123T in yeast have been described previously [30]. Under the conditions used, wild-type Yfh1 was exclusively expressed as a soluble protein, as were most of the mutants. The only exceptions were Yfh1-D86A/E90A/E93A, Yfh1-N122A and Yfh1-N122A/K123/Q124A, in which $\sim$15 % of the expressed protein was found in the insoluble fraction. After harvesting the cells, they were lysed on a French press. Cell lysate was subjected to His-binding resin (GE Healthcare) chromatography and the protein was eluted with 500 mM imidazole in binding buffer (50 mM Tris/HCl, pH 8.0, 200 mM NaCl and 10 mM imidazole). The His_6 tag was cleaved using biotinylated thrombin, and thrombin was removed by streptavidin–agarose (GE Healthcare). When necessary (purity less then 90 %), the protein was purified further by applying the sample on a Superdex 75. At the end, the buffer was changed to 10 mM Hepes and 50 mM NaCl (pH 7.0) using Centricons (Millipore). Protein concentration was determined using the molar absorption coefficient $\varepsilon_{280} = 15470$ $M^{-1} \cdot cm^{-1}$. The mature form of Isu1 (amino acids 35–165) with a His_6 tag and a TEV (tobacco etch virus) protease cleavage site in between was cloned into the pKLD37 vector. Protein expression was induced over 4 h at 30 °C in C41 *E. coli* by adding IPTG at a final concentration of 1 mM. The purification was performed as above described for the Yfh1 variants, but using TEV to cleave the His_6 tag and passing through a His-binding resin to remove it. Protein concentration was determined using the molar absorption coefficient $\varepsilon_{280} = 14161.4$ $M^{-1} \cdot cm^{-1}$.

Spectroscopic methods

UV–visible spectra were recorded at room temperature (20 °C) in a Shimadzu UVPC-1601 spectrometer. Fluorescence spectroscopy was performed on a Cary Varian Eclipse instrument ($\lambda_{ex} = 280$ nm, $\lambda_{em} = 340$ nm, $slit_{ex} = 5$ nm, $slit_{em} = 10$ nm, unless noted otherwise) equipped with cell stirring and Peltier temperature control. Far-UV CD spectra were recorded typically at 0.2 nm resolution on a Jasco J-715 spectropolarimeter fitted with a thermostatically controlled cell holder.

Thermal denaturation

Thermal unfolding was followed by ellipticity ($\Delta\varepsilon_{rmw}$ at 222 nm) variations. In all experiments, a heating rate of 1 °C/min was used, and the temperature was changed from 10 to 90 °C. All reactions were found to be reversible under the conditions used, as inferred from obtaining identical far-UV CD spectra of the proteins before the thermal ramping and after cooling the heated sample; a second temperature ramp of the same sample also yielded identical melting transitions. Protein aggregation was not observed during thermal unfolding. Data were analysed according to a two-state model, and the thermodynamic data parameters were determined [34].

Limited trypsin proteolysis

Frataxins were incubated with trypsin (bovine pancreas trypsin, sequencing grade, Sigma) at 37 °C in 0.1 M Tris/HCl (pH 8.5), in a 150-fold excess over the protease. Aliquots (300 μmol of protein) were sampled at different incubation periods and the reaction was stopped by adding loading buffer with 5 μM BSA, followed by a 10 min incubation at 100 °C. The products of the proteolysis reaction were analysed by SDS/PAGE [35].

Iron-binding assays

Yeast frataxin oligomerizes in an iron-concentration-dependent fashion, but at up to a stoichiometry of two irons per protein, the protein remains in the monomeric form [11,18,23,36]. To avoid side effects from different oligomerization behaviours, we have measured iron binding before oligomerization takes place, i.e. up to an iron/protein ratio of 2. Tryptophan fluorescence emission spectroscopy was used to monitor iron binding, which quenches tryptophan emission as the iron–frataxin complex is being formed. As shown previously, this methods yield results identical with those obtained by isothermal titration calorimetry [16,37]. For the purpose, the quenching of the tryptophan fluorescence ($\lambda_{ex} = 290$ nm; $\lambda_{em} = 340$ nm) of a 50 μM solution of apo-frataxin in 100 mM Hepes (pH 7.0) and 50 mM NaCl was measured upon stepwise addition of an iron citrate solution, in 1 mm-pathlength quartz cuvettes under continuous stirring

[35,37]. These data were used to calculate the fraction of binding sites occupied. The stoichiometry, p, and apparent dissociation constant, K_d, were then determined as described by Winzor and Sawyer [38].

Isu–Yfh1 interaction assay

Holo-Yfh1 was prepared using a stoichiometry of two irons per frataxin to avoid interference from oligomer formation. The formation of a Isu–holo-frataxin complex was followed monitoring the tryptophan fluorescence, taking advantage of the fact that yeast Isu does not contain any tryptophan residues. Thus, when Isu binds to holo-Yfh1, the tryptophan fluorescence emission ($\lambda_{ex} = 290$ nm; $\lambda_{em} = 340$ nm) of the latter is quenched and this can be used to monitor binding. Holo-Yfh1 was prepared in 100 mM Hepes (pH 7.0) and 50 mM NaCl. Aliquots of Isu were added to 2.5 μM holo-frataxins with constant stirring. The stoichiometry, p, and apparent dissociation constant, K_d, were then obtained as described by Winzor and Sawyer [38].

RESULTS AND DISCUSSION

Alterations in the conserved β-sheet surface result in functional effects

To gain a better understanding of the relationship between the structure and function of frataxin, we compared four Yfh1 variants. Three (Yfh1-D101A/E103A, Yfh1-D86A/E90A/E93A and a combination of these two, Yfh1-D86A/E90A/E93A/D101A/E103A) alter the putative iron-binding region at the $\alpha 1/\beta 1$ acidic ridge and oligomerization region (Figure 1). The fourth, Yfh1-N122A/K123T/Q124A (hereafter referred to as Yfh1-122-4), alters the conserved β-sheet, the putative binding surface for interaction with Isu, the scaffold on which Fe–S clusters are built [30]. Since Yfh1 cellular levels can be reduced significantly before any growth defects are detected [39], wild-type and mutant *YFH1* genes were placed under the control of the *tetO* promoter allowing the modulation of protein expression using doxycycline. In this way, *in vivo* function could be tested under both normal and reduced levels of expression. At normal Yfh1 expression levels (without doxycycline), all mutant gene were able to support growth as well as the wild-type gene (Figure 2). In addition, as we reported previously [19,30], Yfh1-122-4 cells grew poorly when the variant was expressed at reduced levels (with doxycycline), whereas cells expressing low levels of Yfh1-D86A/E90A/E93A grew as well as wild-type cells. However, Yfh1-D101A/E103A was slightly compromised, and when these mutations were combined with those of Yfh1-D86A/E90A/E93A, generating alterations in five of the charged residues in the acidic ridge, growth was severely compromised. Consistent with this enhanced growth phenotype, mitochondria isolated from Yfh1-D101A/E103A had lower levels of activity of the Fe–S enzyme aconitase, even when the mutant protein was expressed at normal levels (Figure 3). This effect was more extreme in Yfh1-D86A/E90A/E93A/D101A/E103A mitochondria, which had only 40 % the aconitase activity of wild-type mitochondria. Consistent with the affects on growth, Yfh1-122-4 mitochondria had only 20 % of the aconitase activity quantified for wild-type mitochondria.

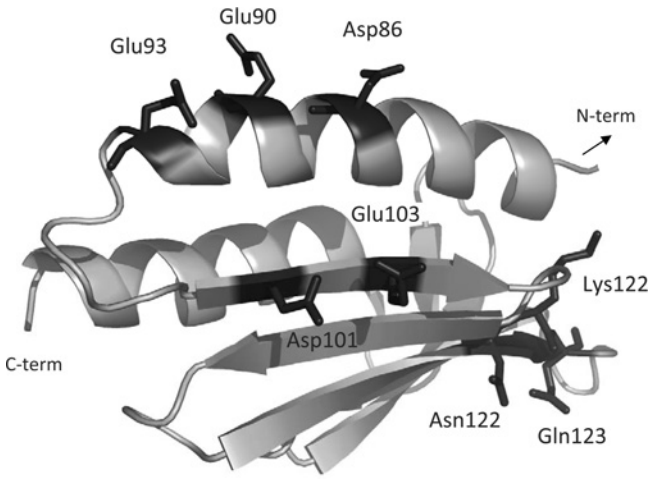

Figure 1 Yfh1 ribbon structure generated using PyMOL (PDB code 2GA5)

Mutated residues are represented by sticks, labelled and highlighted in black. The present study has focused on the structural and conformational characterization of the following variants: Yfh1-D86A/E90A/E93A, Yfh1-D101A/E103A, Yfh1-D86A/E90A/E93A/D101A/E103A, Yfh1-N122A, Yfh1-N122K (corresponding to the human clinical mutation N146K), Yfh1-K123T, Yfh1-Q124A and Yfh1-N122A/K123T/Q124A. term, terminus.

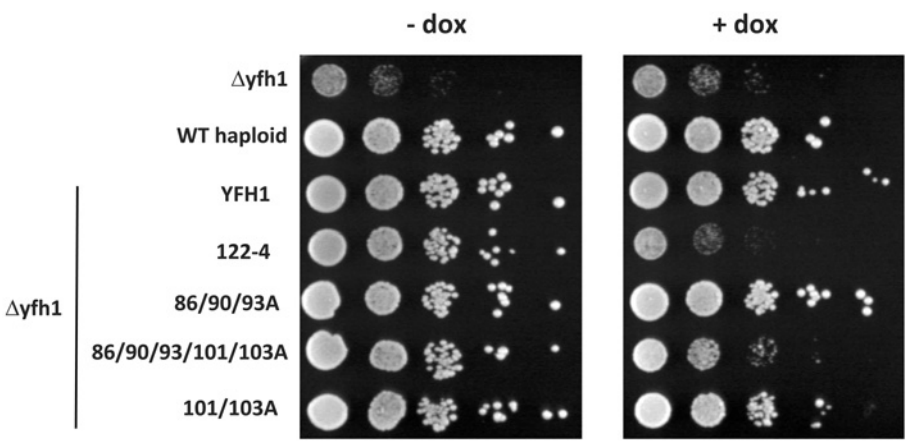

Figure 2 Yeast growth rescue of (Δ*yfh1*) cells by Yfh1 variants

A 10-fold dilutions of cell suspension of wild-type, Δ*yfh1* and Δ*yfh1* transformed with plasmids harbouring the indicated *YFH1* mutant genes under the control of the *tetO*-regulatable wild-type or mutant yfh1 were plated on minimal synthetic medium −ura DO containing (+) or lacking (−) doxycycline (dox). Plates were incubated at 30 °C for 2 days.

Table 1 Thermodynamic parameters for thermal denaturation of yeast frataxin variants

Effect of functional mutations on the protein thermal stability and iron-binding affinity.

Protein	ΔH (kJ · mol^{-1})	ΔG^* (J · mol^{-1})	T_m (°C)	ΔT_m (°C)	$\Delta(\Delta G)$† (J · mol^{-1})	K_d (μM)‡
Wild-type	118.0 ± 1.3	5946.7	40.4 ± 0.1	–	–	10.4 ± 2.1
N122K	145.6 ± 2.1	7772.2	44.7 ± 0.1	+4.3 ± 0.2	2286.6	11.0 ± 3.8
N122A	125.9 ± 1.7	4106.2	35.9 ± 0.1	−4.5 ± 0.2	−2461.5	14.0 ± 1.0
K123T	120.1 ± 1.7	6197.8	41.0 ± 0.1	+0.6 ± 0.2	323.0	18.8 ± 2.4
Q124A	143.5 ± 1.3	5366.0	39.0 ± 0.1	−1.4 ± 0.2	758.1	13.2 ± 3.8
N122A/K123T/Q124A	90.8 ± 1.3	5863.5	40.2 ± 0.1	−0.2 ± 0.2	107.9	27.1 ± 1.0
D101A/E103A	230.5 ± 3.3	11001.4	52.0 ± 0.1	+11.6 ± 0.2	6030.4	20.9 ± 0.6
D86A/E90A/E93A	214.6 ± 3.8	11546.2	53.2 ± 0.1	+12.8 ± 0.2	6630.0	21.3 ± 1.0
D86A/E90A/E93A/D101A/E103A	322.6 ± 6.3	16687.9	64.2 ± 0.1	+23.8 ± 0.2	11925.2	22.8 ± 0.9

*ΔG at 25 °C, considering an estimate for ΔC_p of 50.2 J/mol per K.
†$\Delta(\Delta G) = [\Delta(T_m)] \times \Delta S_m = [\Delta(T_m)] \times (\Delta H_m/T_m)$, where ΔS_m and ΔH_m are values for the wild-type.
‡ $n = 2$.

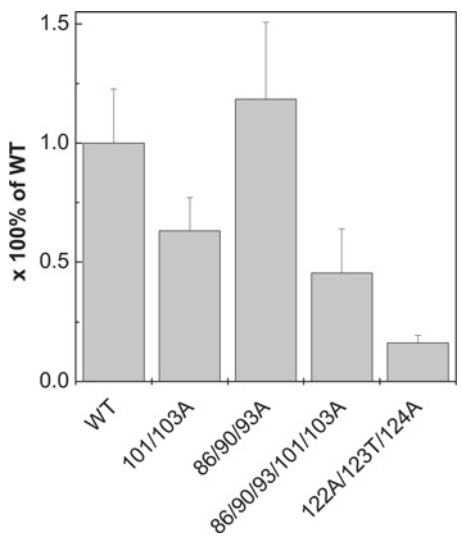

Figure 3 Aconitase activity

Extracts (150 μg) from mitochondria isolated from the indicated strains were prepared, and aconitase activity was measured. Results are mean ± S.E.M. percentages of wild-type (WT) aconitase activity ($n = 3$).

None of the mutations abolishes iron binding

Since iron binding is an essential functional feature of frataxin, we asked whether iron-binding properties of the Yfh1 variants were affected. In order to exclude iron-induced frataxin oligomerization effects, we have investigated iron binding at low stoichiometry [up to two Fe(II)/Yfh1], i.e. under conditions in which oligomerization does not take place. We have used tryptophan fluorescence to monitor iron binding to Yfh1 variants, as tryptophan emission is a specific reporter for iron binding to frataxin. Our measurements indicated that mutations altering the iron-binding region, D86A, E93A, D101A and E103A, had no effect on the iron-binding capacity at low stoichiometry, but did decrease binding affinity somewhat (Table 1). Conversely, iron must be able to bind to frataxin through other residues, as even the quintuple mutant Yfh1-D86A/E90A/E93A/D101A/E103A retained the ability to bind ~2 Fe(II)/Yfh1. We hypothesize that iron is binding to secondary sites with lower affinity, as evident by the higher dissociation constants (~20 μM). In fact, a previous NMR study has shown that, under identical conditions at low iron stoichiometry, iron binding to Yfh1 affected multiple sites: mainly interactions with carboxy groups and nitrogen from acidic residues within the $\alpha 1/\beta 1$ ridge (His^{83}, Asp^{86}, Glu^{93}, His^{95}, Asp^{101} and Glu^{103}), but other residues (Ala^{94}, Leu^{104}, Ser^{105} and Asn^{140}) were also found to change their resonance positions upon binding of up to two irons per frataxin [23]. The lower binding affinity that we have determined in the Yfh1 variants (nevertheless still in the micromolar range comparable with that of human frataxins) could possibly indicate the recruitment of secondary positions, rather than unspecific binding. However, this is not the case, as the observed iron binding is functional, as shown by the fact that yeast expressing these variants still has some aconitase activity (Figure 3), which depends on frataxin-mediated iron transfer [15]. In addition, a previous study confirms our observations: it has been shown that single point mutations to alanine on residues 86, 90, 93, 101 and 103 reduce Yfh1 affinity for iron, but do not abolish iron binding [24]. Single point mutations in the Asn^{122}–Gln^{124} segment seem to have an intermediate effect in respect to the binding affinity (~14–18 μM). Presumably, alterations in the protein–protein interaction region of Yfh1 result in long-range effects on the iron-binding acid ridge leading to a decrease in the iron-binding affinity.

Isu binding may also involve residues from the acidic ridge

Since low-stoichiometric iron binding was not impaired in the mutants, we next evaluated whether the interaction between Yfh1 and Isu was compromised. This interaction is mediated by iron, as only holo-Yfh1 interacts with Isu [16]. Yfh1-D86A/E90A/E93A was found to bind to Isu with a wild-type-like affinity (K_d ~5 μM), whereas no interaction with Yfh1-122-4 was detected, consistent with previously published results ([19] and [30] respectively). The alteration of residues 122, 123 and 124 individually (N122K, N122A, K123T or Q124A) severely affected the Isu interaction, supporting the hypothesis that all three residues are important for this interaction.

No interaction between Isu and Yfh1-D101A/E103A (or Yfh1-D86A/E90A/E93A/D101A/E103A) was detected in our *in vitro* assay. This reduced interaction is somewhat surprising considering that Yfh1-D101A/E103A could significantly rescue the growth defect of *Δyfh1* cells, even when expressed at low levels (Figure 2). Mutating these two residues has only been found to cause a growth defect when the alterations are to lysine residues and the medium is supplemented with high levels of iron [20]. *In vivo*, other cellular factors may promote the interaction between Yfh1-D101A/E103A and Isu, explaining the difference between the *in vivo* and *in vitro*

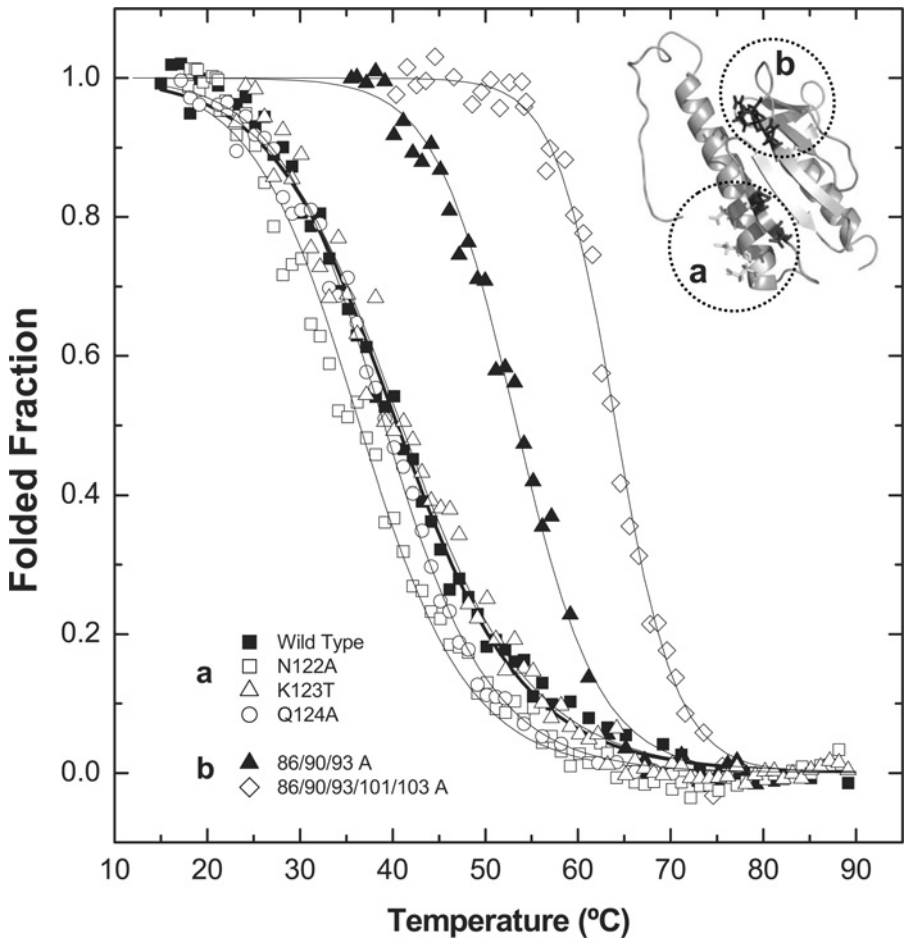

Figure 4 Thermal denaturation curves at pH 7.0 following tryptophan emission: impact of mutations on Yfh1 thermal stability

(■) Wild-type and (a) single point mutations of β-sheet surface residues (122–123): (□) N122A, (△) K123T and (○) Q124A. (b) Mutations on putative iron-binding sites: (▲) D86A/E90A/E93A and (◇) D86A/E90A/E93A/D101A/E103A. Lines represent fits to the two-state model described in [34]; for parameters see Table 1.

results. Indeed, frataxin was found to interact with Isd11 of the Nfs1–Isu complex and multiple mitochondrial chaperones [40]. Alternatively, significantly reduced affinity may be tolerated *in vivo*.

Charge-to-neutral alterations in the $\alpha 1/\beta 1$ acidic ridge increase stability

In order to evaluate whether the functional impairment may result from decreased protein stability, the effect of the alterations on Yfh1 folding thermodynamics was analysed by comparing the thermal stability of mutant variants with that of wild-type. According to the analysis of the far-UV CD spectra at 20 °C, before and after thermal denaturation, thermal unfolding was reversible for all protein variants studied and no aggregation was observed after thermal unfolding. The results showed that charge-to-neutral alterations in the acidic ridge result in an impressive stabilization of the protein fold: an increase of up to $\sim$24 °C was noted for the Yfh1-D86A/E90A/E93A/D101A/E103A variant, whereas alterations in the β-sheet surface had almost no effect on protein thermal stability (Figure 4 and Table 1).

The protein stability decreased in the order: Yfh1-D86A/E90A/E93A/D101A/E103A>Yfh1-D86A/E90A/E93A>Yfh1-D101A/E103A>Yfh1-N122K>Yfh1-K123T>wild-type>Yfh1-N122A/K123T/Q124A>Yfh1-Q124A>Yfh1-N122A. The exceptions to the effect on the β-sheet surface are the mutations in Asn^{122}: changing to an alanine ($\Delta T_m = -4.5$ °C) or to a lysine ($\Delta T_m = +4.3$ °C) residue had opposite effects, probably due to the effect these alterations would be expected to have on the β-hairpin between strands $\beta 3$ and $\beta 4$, which involves two hydrogen bonds (Asn^{122}–Trp^{131} and Val^{120}–Ala^{133}). Whereas the insertion of an alanine residue probably disrupts the hydrogen bond with Trp^{131}, the positively charged lysine residue might strengthen it, stabilizing the protein. The D101A/E103A alterations stabilize the protein in spite of compromising two of the three hydrogen bonds involved in the β-hairpin connecting strands $\beta 1$ and $\beta 2$. This suggests that minimizing repulsive interactions overcomes the stabilization obtained by the two hydrogen bonds.

Since protein conformational plasticity affects both protein function and degradation rates, we next analysed whether the functional mutations were also affecting frataxin flexibility, by performing limited proteolysis experiments using trypsin. Our underlying rationale was that mutations resulting in an increased structural flexibility would increase trypsin access to cleavage sites and consequently increase the degradation rate. The results show two distinct patterns, depending on the region in which the alteration is located (Figure 5). Alterations on the acidic ridge had a pronounced effect on frataxin dynamics, making the protein more rigid and substantially less susceptible to proteolysis. In fact, the Yfh1-D86A/E90A/E93A/D101A/E103A

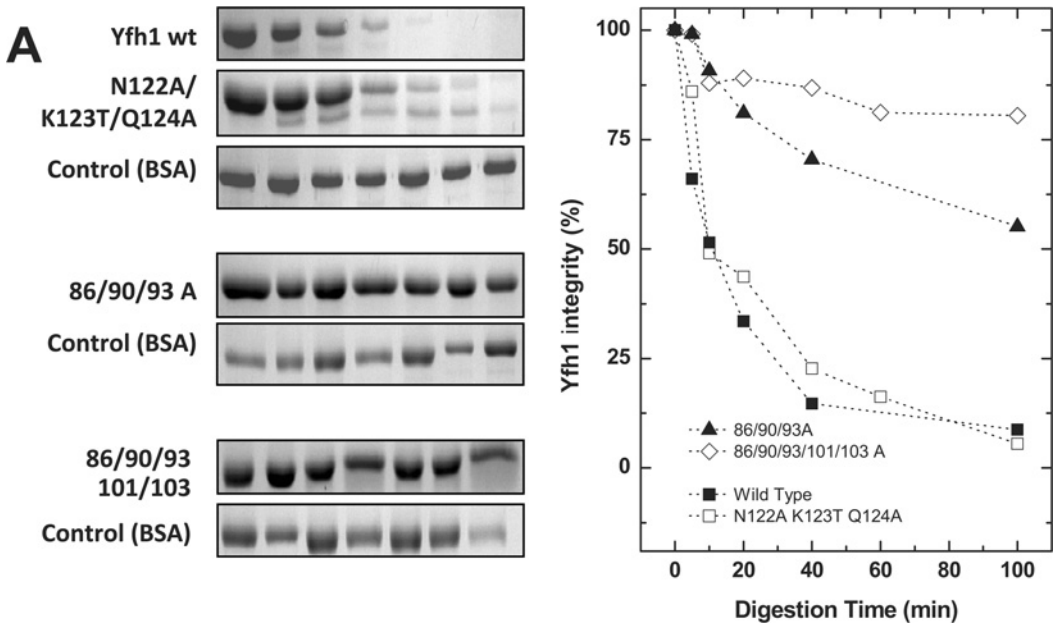

Figure 5 Time course of limited trypsin proteolysis

Comparison between wild-type and functional mutants. (**A**) SDS/PAGE analysis of the time course of limited trypsin proteolysis experiments. (**B**) Evaluation/quantification of frataxin degradation during incubation with trypsin. Densitometric analysis of gels in (**A**) allowed the quantification of frataxin for the different incubation times with trypsin. (■) Wild-type, (□) N122A/K123T/Q124A, (▲) D86A/E90A/E93A and (◇) D86A/E90A/E93A/D101A/E103A.

variant remains essentially intact under conditions in which wild-type frataxin is essentially completely digested (80 % compared with 10 % integrity after 100 min of digestion). On the other hand, alterations on the β-sheet surface (Yfh1-N122A/K123T/Q124A) behave almost identically with the wild-type, suggesting that modifications in this region have either a very small or no effect on the protein conformational plasticity.

Overall, alterations in the acidic ridge that prevent iron binding at the primary sites increased substantially the protein stability, and decreased its flexibility. Decreases in the structural flexibility may prevent conformational changes necessary to allow the interaction with protein partners. This increase in both thermal stability and resistance to proteolytic degradation suggests that the iron-binding region is particularly susceptible to an activity–stability trade off.

Conclusions

In the present paper, we describe a detailed characterization of eight yeast frataxin functional variants that either alter the acidic ridge between α-helix 1 and β-sheet 1, or the conserved β-sheet surface between strands 3 and 4. Changing the conserved β-sheet residues Asn^{122}–Lys^{123}–Gln^{124} had almost no effect on Yfh1 stability and plasticity, indicating that changes in this region did not disrupt overall conformation, but are relevant for the Yfh1–Isu interaction. Alteration of up to five residues in the acidic ridge region, four of which had been identified as iron-binding sites [23], significantly increased frataxin stability. Thus illustrates a rather interesting trade off between activity and stability in this region. In addition, the present study suggests that residues Asp^{101} and Glu^{103} are involved in the iron-mediated interaction between Isu and Yfh1, but their alteration does not abrogate the interaction, as is evident by the rescue of the $\Delta yfh1$ phenotype.

AUTHOR CONTRIBUTION

Ana Correia and Tao Wang designed and performed experiments, analysed data and wrote the paper. Elizabeth Craig and Cláudio Gomes conceived the study, designed experiments, analysed data and wrote the paper.

FUNDING

This work was partly financed by the Fundação para a Ciência e Tecnologia [grant number PTDC/QUI/70101], National Ataxia Foundation (to C. M. G.), the National Institutes of Health [grant number GM27870] and Muscular Dystrophy Association (to E. A. C.). A. R. C. and T. W. were recipients of a Fundação para a Ciência e Tecnologia Ph.D. Fellowship [grant number SFRHBD/24949/2005] and an American Heart Association Postdoctoral Fellowship [grant number 0525728Z] respectively.

REFERENCES

1 Pandolfo, M. (2009) Friedreich ataxia: the clinical picture. J. Neurol. **256** (Suppl. 1), 3–8
2 Becker, E. and Richardson, D. R. (2001) Frataxin: its role in iron metabolism and the pathogenesis of Friedreich's ataxia. Int. J. Biochem. Cell Biol. **33**, 1–10
3 Durr, A. and Brice, A. (2000) Clinical and genetic aspects of spinocerebellar degeneration. Curr. Opin. Neurol. **13**, 407–413
4 Puccio, H. (2009) Multicellular models of Friedreich ataxia. J. Neurol. **256** (Suppl. 1), 18–24
5 Huang, M. L., Becker, E. M., Whitnall, M., Rahmanto, Y. S., Ponka, P. and Richardson, D. R. (2009) Elucidation of the mechanism of mitochondrial iron loading in Friedreich's ataxia by analysis of a mouse mutant. Proc. Natl. Acad. Sci. U.S.A. **106**, 16381–16386
6 Richardson, D. R. (2003) Friedreich's ataxia: iron chelators that target the mitochondrion as a therapeutic strategy? Expert Opin. Investig. Drugs **12**, 235–245
7 Herman, D., Jenssen, K., Burnett, R., Soragni, E., Perlman, S. L. and Gottesfeld, J. M. (2006) Histone deacetylase inhibitors reverse gene silencing in Friedreich's ataxia. Nat. Chem. Biol. **2**, 551–558
8 Schulz, J. B., Boesch, S., Burk, K., Durr, A., Giunti, P., Mariotti, C., Pousset, F., Schols, L., Vankan, P. and Pandolfo, M. (2009) Diagnosis and treatment of Friedreich ataxia: a European perspective. Nat. Rev. Neurol. **5**, 222–234

9 Babcock, M., de Silva, D., Oaks, R., Davis-Kaplan, S., Jiralerspong, S., Montermini, L., Pandolfo, M. and Kaplan, J. (1997) Regulation of mitochondrial iron accumulation by Yfh1p, a putative homolog of frataxin. Science **276**, 1709–1712

10 Rotig, A., de Lonlay, P., Chretien, D., Foury, F., Koenig, M., Sidi, D., Munnich, A. and Rustin, P. (1997) Aconitase and mitochondrial iron–sulphur protein deficiency in Friedreich ataxia. Nat. Genet. **17**, 215–217

11 Gakh, O., Adamec, J., Gacy, A. M., Twesten, R. D., Owen, W. G. and Isaya, G. (2002) Physical evidence that yeast frataxin is an iron storage protein. Biochemistry **41**, 6798–6804

12 Schulz, J. B., Dehmer, T., Schols, L., Mende, H., Hardt, C., Vorgerd, M., Burk, K., Matson, W., Dichgans, J., Beal, M. F. and Bogdanov, M. B. (2000) Oxidative stress in patients with Friedreich ataxia. Neurology **55**, 1719–1721

13 Thierbach, R., Schulz, T. J., Isken, F., Voigt, A., Mietzner, B., Drewes, G., von Kleist-Retzow, J. C., Wiesner, R. J., Magnuson, M. A., Puccio, H. et al. (2005) Targeted disruption of hepatic frataxin expression causes impaired mitochondrial function, decreased life span and tumor growth in mice. Hum. Mol. Genet. **14**, 3857–3864

14 Vazquez-Manrique, R. P., Gonzalez-Cabo, P., Ros, S., Aziz, H., Baylis, H. A. and Palau, F. (2006) Reduction of *Caenorhabditis elegans* frataxin increases sensitivity to oxidative stress, reduces lifespan, and causes lethality in a mitochondrial complex II mutant. FASEB J. **20**, 172–174

15 Bulteau, A. L., O'Neill, H. A., Kennedy, M. C., Ikeda-Saito, M., Isaya, G. and Szweda, L. I. (2004) Frataxin acts as an iron chaperone protein to modulate mitochondrial aconitase activity. Science **305**, 242–245

16 Yoon, T. and Cowan, J. A. (2003) Iron–sulfur cluster biosynthesis: characterization of frataxin as an iron donor for assembly of [2Fe–2S] clusters in ISU-type proteins. J. Am. Chem. Soc. **125**, 6078–6084

17 Yoon, T. and Cowan, J. A. (2004) Frataxin-mediated iron delivery to ferrochelatase in the final step of heme biosynthesis. J. Biol. Chem. **279**, 25943–25946

18 Adamec, J., Rusnak, F., Owen, W. G., Naylor, S., Benson, L. M., Gacy, A. M. and Isaya, G. (2000) Iron-dependent self-assembly of recombinant yeast frataxin: implications for Friedreich ataxia. Am. J. Hum. Genet. **67**, 549–562

19 Aloria, K., Schilke, B., Andrew, A. and Craig, E. A. (2004) Iron-induced oligomerization of yeast frataxin homologue Yfh1 is dispensable *in vivo*. EMBO Rep. **5**, 1096–1101

20 Foury, F., Pastore, A. and Trincal, M. (2007) Acidic residues of yeast frataxin have an essential role in Fe–S cluster assembly. EMBO Rep. **8**, 194–199

21 Cook, J. D., Bencze, K. Z., Jankovic, A. D., Crater, A. K., Busch, C. N., Bradley, P. B., Stemmler, A. J., Spaller, M. R. and Stemmler, T. L. (2006) Monomeric yeast frataxin is an iron-binding protein. Biochemistry **45**, 7767–7777

22 Kondapalli, K. C., Kok, N. M., Dancis, A. and Stemmler, T. L. (2008) *Drosophila* frataxin: an iron chaperone during cellular Fe–S cluster bioassembly. Biochemistry **47**, 6917–6927

23 He, Y., Alam, S. L., Proteasa, S. V., Zhang, Y., Lesuisse, E., Dancis, A. and Stemmler, T. L. (2004) Yeast frataxin solution structure, iron binding, and ferrochelatase interaction. Biochemistry **43**, 16254–16262

24 Gakh, O., Park, S., Liu, G., Macomber, L., Imlay, J. A., Ferreira, G. C. and Isaya, G. (2006) Mitochondrial iron detoxification is a primary function of frataxin that limits oxidative damage and preserves cell longevity. Hum. Mol. Genet. **15**, 467–479

25 Cho, S. J., Lee, M. G., Yang, J. K., Lee, J. Y., Song, H. K. and Suh, S. W. (2000) Crystal structure of *Escherichia coli* CyaY protein reveals a previously unidentified fold for the evolutionarily conserved frataxin family. Proc. Natl. Acad. Sci. U.S.A. **97**, 8932–8937

26 Dhe-Paganon, S., Shigeta, R., Chi, Y. I., Ristow, M. and Shoelson, S. E. (2000) Crystal structure of human frataxin. J. Biol. Chem. **275**, 30753–30756

27 Musco, G., de Tommasi, T., Stier, G., Kolmerer, B., Bottomley, M., Adinolfi, S., Muskett, F. W., Gibson, T. J., Frenkiel, T. A. and Pastore, A. (1999) Assignment of the ^{1}H, ^{15}N, and ^{13}C resonances of the C-terminal domain of frataxin, the protein responsible for Friedreich ataxia. J. Biomol. NMR **15**, 87–88

28 Nair, M., Adinolfi, S., Pastore, C., Kelly, G., Temussi, P. and Pastore, A. (2004) Solution structure of the bacterial frataxin ortholog, CyaY: mapping the iron binding sites. Structure **12**, 2037–2048

29 Musco, G., Stier, G., Kolmerer, B., Adinolfi, S., Martin, S., Frenkiel, T., Gibson, T. and Pastore, A. (2000) Towards a structural understanding of Friedreich's ataxia: the solution structure of frataxin. Structure **8**, 695–707

30 Wang, T. and Craig, E. A. (2008) Binding of yeast frataxin to the scaffold for Fe–S cluster biogenesis, Isu. J. Biol. Chem. **283**, 12674–12679

31 Gari, E., Piedrafita, L., Aldea, M. and Herrero, E. (1997) A set of vectors with a tetracycline-regulatable promoter system for modulated gene expression in *Saccharomyces cerevisiae*. Yeast **13**, 837–848

32 Li, J., Kogan, M., Knight, S. A., Pain, D. and Dancis, A. (1999) Yeast mitochondrial protein, Nfs1p, coordinately regulates iron–sulfur cluster proteins, cellular iron uptake, and iron distribution. J. Biol. Chem. **274**, 33025–33034

33 Murakami, H., Pain, D. and Blobel, G. (1988) 70-kD heat shock-related protein is one of at least two distinct cytosolic factors stimulating protein import into mitochondria. J. Cell Biol. **107**, 2051–2057

34 Pace, C. N., Hebert, E. J., Shaw, K. L., Schell, D., Both, V., Krajcikova, D., Sevcik, J., Wilson, K. S., Dauter, Z., Hartley, R. W. and Grimsley, G. R. (1998) Conformational stability and thermodynamics of folding of ribonucleases Sa, Sa2 and Sa3. J. Mol. Biol. **279**, 271–286

35 Correia, A. R., Pastore, C., Adinolfi, S., Pastore, A. and Gomes, C. M. (2008) Dynamics, stability and iron-binding activity of frataxin clinical mutants. FEBS J. **275**, 3680–3690

36 Bencze, K. Z., Kondapalli, K. C., Cook, J. D., McMahon, S., Millan-Pacheco, C., Pastor, N. and Stemmler, T. L. (2006) The structure and function of frataxin. Crit. Rev. Biochem. Mol. Biol. **41**, 269–291

37 Correia, A. R., Adinolfi, S., Pastore, A. and Gomes, C. M. (2006) Conformational stability of human frataxin and effect of Friedreich's ataxia-related mutations on protein folding. Biochem. J. **398**, 605–611

38 Winzor, D. J. and Sawyer, W. H. (1995) Quantitative Characterisation of Ligand Binding, Wiley-Liss, New York

39 Karthikeyan, G., Santos, J. H., Graziewicz, M. A., Copeland, W. C., Isaya, G., Van Houten, B. and Resnick, M. A. (2003) Reduction in frataxin causes progressive accumulation of mitochondrial damage. Hum. Mol. Genet. **12**, 3331–3342

40 Shan, Y., Napoli, E. and Cortopassi, G. (2007) Mitochondrial frataxin interacts with ISD11 of the Nfs1/ISCU complex and multiple mitochondrial chaperones. Hum. Mol. Genet. **16**, 929–941

Received 19 October 2009/24 November 2009; accepted 14 December 2009
Published as BJ Immediate Publication 14 December 2009, doi:10.1042/BJ20091612